

Research Article

Calycosin Ameliorates Bleomycin-Induced Pulmonary Fibrosis via Suppressing Oxidative Stress, Apoptosis, and Enhancing Autophagy

Haoge Liu ¹, Xiaoxu Bai,² Wan Wei,³ Zhipeng Li,¹ Zhengju Zhang,¹ Weili Tan,¹ Bin Wei,¹ Hantao Zhao,¹ and Yang Jiao ⁴

¹Graduate School, Beijing University of Chinese Medicine, Beijing, China

²Department of Respiratory, Fangshan Hospital Affiliated to Beijing University of Chinese Medicine, Beijing, China

³Department of Geratology, Dongfang Hospital Affiliated to Beijing University of Chinese Medicine, Beijing, China

⁴Department of Respiratory, Dongfang Hospital Affiliated to Beijing University of Chinese Medicine, Beijing, China

Correspondence should be addressed to Yang Jiao; yangjiao2013@sina.cn

Received 20 June 2022; Revised 12 September 2022; Accepted 14 September 2022; Published 11 October 2022

Academic Editor: Chen-Huan Yu

Copyright © 2022 Haoge Liu et al. This is an open access article distributed under the Creative Commons Attribution License, which permits unrestricted use, distribution, and reproduction in any medium, provided the original work is properly cited.

Calycosin (CA) is a flavonoid extracted from the root of *Astragalus membranaceus* and has antioxidant, anti-inflammation, and antiapoptosis properties. The objective of this study was to investigate the efficacy of CA in protecting against pulmonary fibrosis. CA (14 mg/kg) and SB216763 (20 mg/kg) were administered to bleomycin-induced pulmonary fibrosis mice for 3 weeks. The results concluded that CA alleviated the inflammation and collagen deposition in pulmonary fibrosis. In addition, CA reduced MDA level, enhanced SOD and TAC activities, and increased the activity of the Nrf2/HO-1 pathway. CA also regulated the expressions of apoptosis-related proteins. Moreover, CA enhanced autophagy via upregulating LC3, beclin1, PINK1, and reducing p62. CA also increased expression of LAMP1 and TFEB, and inhibited the release of lysosome enzymes from ruptured lysosomes. These results provide new evidence that CA protects against pulmonary fibrosis through inhibiting oxidative stress and apoptosis. In addition, autophagy abnormality and lysosome dysfunction are restored by CA.

1. Introduction

Idiopathic pulmonary fibrosis (IPF) is a devastating lung disease of unknown aetiology characterized by progressive fibrosing interstitial pneumonitis, fibroblast proliferation, and excessive extracellular matrix production [1]. The median survival duration of IPF averages to 3–5 years after diagnosis. IPF occurs primarily in the elderly men, and most patients have a history of smoking. Although nintedanib and pirfenidone are currently approved by the Food and Drug Administration as pharmacological therapies for IPF, neither of them can improve survival rates among patients with IPF [2, 3]. Lung transplantation is the only cure for IPF patients. There is an urgent need to find new therapeutic drugs for IPF treatment. The lung is a delicate and essential organ directly exposed to air and its

constituent pathogens, airborne irritants, and hazardous pollutants. Oxidative stress contributes to pulmonary fibrosis by multiple mechanisms. Hyperoxia-induced oxidative damage results in alveolar epithelial cell apoptosis [4]. Mitochondrial reactive oxygen species (mtROS) generation by mitochondrial complex III has been shown to enhance the process of differentiation into the myofibroblast phenotype [5]. Studies identified that intermittent hypoxia-mediated oxidative stress accentuated bleomycin (BLM)-induced pulmonary fibrosis [6]. The genetic knockout of Nrf2 exacerbates experimental pulmonary fibrosis of mice. In addition, the activation of Nrf2/HO-1 pathway suppresses epithelial-mesenchymal transition in pulmonary epithelial cells [7]. Thus, targeting the oxidative stress may serve as a therapeutic strategy for pulmonary fibrosis.

Autophagy is a process that relies on lysosomes to degrade damaged organelles or proteins. Mitochondrial autophagy is a selective form of autophagy. The inactivation of autophagy results in the accumulation of proteins and morphologically abnormal mitochondria [8]. In addition, ROS leads to mitochondrial damage, which in turn leads to more ROS release. Therefore, aberrant autophagy is suggested as a pathological driver of pulmonary fibrosis [9]. A previous study indicated that impaired autophagy was observed in the lungs of BLM-treated mice [10]. Moreover, *Atg4b* gene deletion exacerbated collagen accumulation and promoted excessive extracellular matrix-related gene expression [11]. Targeting autophagy may be an effective approach for inhibiting pulmonary fibrosis. Kim et al. reported that interleukin-37 inhibited oxidative stress-induced alveolar epithelial cell (AEC) death via transforming growth factor- β 1 signaling through enhancement of autophagy [12]. Kurita et al. suggested that pirfenidone inhibited the myofibroblast differentiation through autophagy/mitophagy activation and reducing mitochondrial ROS via PDGFR-PI3K-Akt pathway [5].

The aetiology and molecular mechanisms of pulmonary fibrosis is not well elucidated. Considerable attention has been invested in the search for novel efficient natural drugs of plant origin for pulmonary fibrosis. Calycosin, one of the flavonoids, is extracted from the root of *Astragalus membranaceus*. It was previously demonstrated that CA could attenuate pulmonary fibrosis [13]. One study indicated that after the oral administration of pulmonary rehabilitation mixture (124.4 μ g/g of CA), the AUC_{0-t} , $AUC_{0-\infty}$, and $t_{1/2}$ of CA in pulmonary fibrosis rats increased markedly compared to normal rats [14]. Calycosin has the potential to be developed into an antifibrotic drug. However, the specific therapeutic mechanism of CA requires further investigations. In this study, BLM was used to establish rodent models to mimic the pathologic features of pulmonary fibrosis. We aimed to evaluate whether CA could mitigate BLM-induced pulmonary fibrosis by reducing oxidative stress and regulating apoptosis and autophagy.

2. Materials and Methods

2.1. Chemicals and Regent. Calycosin was obtained from Chengdu Must Bio-Technology Co., Ltd. (Chengdu, China; cat: A0514); its purity was $\geq 99\%$. Bleomycin was supplied by Fresenius Kabi (Lake Zurich, USA). SB216763 (SB) was purchased from MedChem Express (Shanghai, China; cat: HY-12012).

2.2. Animals. All mice experiments were approved by and performed in accordance with the guidelines of the Animal Experimental Ethical Committee of Beijing University of Chinese Medicine. This study included 40 C57BL male mice weighing 22 ± 2 g each. The seven-week-old mice were purchased from Beijing Vital River Laboratory Animal Technology Co., Ltd. (Beijing, China). The mice were housed under laboratory conditions. The temperature was kept at

22–26°C, and the ambient humidity was kept at 50%–60%. Food and water were freely available to the mice.

2.3. Animal Treatment. Forty mice were randomly divided into 4 groups: normal control (NC) group, BLM group, CA group, and SB group. After one week of adaptive feeding, the mice were all anesthetized with isoflurane inhalation (5% isoflurane induction) to modelling. Except for the NC group, all mice were instilled BLM (2 U/kg) solution from the airway as described previously [15]. The NC group was administered the same amount of physiological saline. One day later, the mice in each group were treated as follows.

NC and BLM groups: mice were administered with physiological saline by gavage once a day for 21 days and the vehicle (25% dimethyl sulfoxide, 25% polyethylene glycol, and 50% saline) was administered by intraperitoneal injection twice a week.

CA group: mice were administered with CA (14 mg/kg) [13] by gavage once a day for 21 days and the vehicle (25% dimethyl sulfoxide, 25% polyethylene glycol, and 50% saline) was administered by intraperitoneal injection twice a week.

SB group: mice were administered with physiological saline by gavage once a day for 21 days and SB216763 (20 mg/kg) dissolved in the vehicle was administered by intraperitoneal injection twice a week [16]. SB216763, one of the glycogen synthase kinase 3 β inhibitor, can promote autophagy and inhibit apoptosis [17].

The body weight of each mouse was measured every 3 days. All mice were euthanized using isoflurane at the end of 21 days.

2.4. Histological Staining. For hematoxylin-eosin (HE) staining, the left lung samples were fixed immediately with 4% paraformaldehyde, paraffin-embedded, and sectioned at 4 μ m. The sections were then counterstained with hematoxylin (15 min) and eosin (5 min). The tissue sections were stained with Masson using the corresponding kit (Solarbio Life Sciences, Beijing, China). Semiquantitative analysis of inflammation was performed using Alveolitis and Ashcroft scores, respectively. The area of positive staining for Masson trichrome was measured, and then compared to the total area as a ratio using ImageJ software (ImageJ Software Inc., Maryland, USA).

2.5. Immunohistochemistry Analysis. Immunohistochemistry was performed as previously described [18]. In short, after dewaxing and rehydration, the slides were immersed in microwave-pretreated boiling citrate buffer (0.01 M, pH 8.0) for antigen repair. After cooling at room temperature (21°C), 3% H₂O₂ was added to deactivate endogenous peroxidase. The slides were washed in phosphate buffer solution and incubated with blocking serum (10% nonimmune goat serum) to block nonspecific immunolabeling at room temperature (21°C). Primary antibodies were incubated with the slides overnight at 4°C. Slides were then incubated with the appropriate secondary antibodies. After rinsing with phosphate buffer solution, the sections were visualized with

diaminobenzidine and counterstained with hematoxylin. Neutral gum was used for sealing, and all the sections were photographed under an Olympus BX50F4 light microscope (Olympus, Center Valley, PA).

2.6. Superoxide Dismutase (SOD), Total Antioxidant Capacity (TAC), and Malondialdehyde (MDA) Measurements. Serum was separated by low-speed centrifugation (3000 r/min) for 15 minutes. The levels of MDA, SOD, and TAC in serum were detected with an automatic analyzer (Biochemical analyzer BS-200, Mindray, China). The operation process was carried out according to the manufacturer's instructions.

2.7. Western Blot Assay. Briefly, lung tissues were homogenized and the proteins were extracted in tissue lysis buffer. Total proteins were quantified with bicinchoninic acid protein assay kits (MD913053; MDL, Beijing, China) following the manufacturer's instructions. 20 μ g proteins per sample were separated by sodium dodecyl sulfate-polyacrylamide gel electrophoresis on 10% gels and transferred to polyvinylidene difluoride membranes. The membrane was blocked for 2 hours by 5% skimmed milk in Tris-buffered saline at room temperature (21°C). For antibody staining, samples were incubated with primary antibodies at 4°C overnight including anti-LC3A/B (Affinity, AF5402, 1:1000), anti-SQSTM1/p62 (Affinity, AF5384, 1:1000), anti-Becclin 1 (Affinity, AF5384, 1:1000), anti-LAMP1 (Affinity, AF5182, 1:1000), anti-HO-1 (Affinity, DF7033, 1:1000), anti-PINK1 (Affinity, AF5393, 1:1000), goat anti-rabbitIgG-HRP (Affinity, S0001, 1:1000), goat anti-rabbitIgG-FITC (Affinity, S0008, 1:1000), rabbit anti-collagen α -1 (Bioss, bs-20124R, 1:1000), and rabbit anti-Legumain (Bioss, bs-3907R, 1:1000). Membranes were incubated with appropriate secondary antibody (MDL, MD932477, 1:10,000) for 1 hour at room temperature (21°C). The protein bands were visualized by using the enhanced chemiluminescence detection system (ThermoFisher, Waltham, MA) and were quantified using a ChemiDoc Imaging System (Bio-Rad, USA). All of the determinations were performed independently and repeated three times.

2.8. Transmission Electron Microscopy. Transmission electron microscopy (TEM) was performed to observe the autophagy-related structure. Lung tissues were post-fixed in 1% osmium tetroxide for 3 hours. After dehydration with graded ethanol and acetone, samples were embedded in Spurr, sliced into 70 nm thick pieces, stained with uranyl acetate and lead citrate, and observed using TEM (JEM-1400, JEOL, Tokyo, Japan). The number of autolysosomes was evaluated at 20,000 \times .

2.9. RNA Isolation and Quantitative Real-Time Polymerase Chain Reaction (PCR) Analysis. Total RNA was extracted using Trizol (cat. No. 10296028, TRIzol, Invitrogen) following manufacturer's instructions. The RNA concentration and purity were determined using an Eppendorf

Biophotometer (Eppendorf Company, Hamburg, Germany). The total RNA was then converted into cDNA using Superscript III RT-PCR kit (Invitrogen, cat no. 11752050). The primers used were as follows: Nrf2: forward 5'-ACTCAAATCCCACCTTAAACAC-3', reverse 5'-GTCACAGCCTTCAATAGTCCC-3'; XIAP: forward 5'-ATATGAGCACGGATCGTTA-3', reverse 5'-CTCCTCCACAGTGAAAGCA-3'; Bax: forward 5'-AGGGTTTCATCCAGATCGAGCA-3', reverse 5'-CAGCTTCTTGGTGGACGCATC-3'; Bcl-2: forward 5'-ACTTCTCTCGTCGCTACC GTC-3', reverse 5'-CCCCATCCCTGAAGAGTTCCT-3'; TFEB: forward 5'-AGTGGTCTTGGGCAAATCCCTTCT-3', reverse 5'-TGGTTCGGGCTCCCTGTAGTCG-3'; β -actin: forward 5'-CCAGCCTTCCTTCTTGGGTA-3', reverse 5'-CAATGCCTGGGTACATGGTG-3'. β -actin was chosen as a control, and gene expression levels were quantified by the $2^{-\Delta\Delta CT}$ method.

2.10. Statistical Analysis. Statistical analysis was performed using GraphPad Prism 8.0 software (GraphPad Software, San Diego, USA). The data were presented as mean \pm SD. One-way ANOVA followed by Tukey's post hoc test were used for intragroup and intergroup comparisons. Any difference was considered significant when $P < 0.05$.

3. Results

3.1. The Effect of CA on BLM-Induced Pulmonary Fibrosis. To explore the effect of CA on pulmonary fibrosis, lung tissues were analyzed by HE and Masson staining. In Figure 1(a), HE showed severe damage of lung structure after BLM administration. The walls of the alveoli and the alveolar septum were thickened and a large degree of inflammatory cell infiltration was observed. Calycosin and SB treatment attenuated these changes, while the lung injury score ($P < 0.01$) and Ashcroft score ($P < 0.01$) were significantly decreased (Figures 1(d) and 1(e)). Masson staining showed that interstitial fibrosis and disruption of lung structure occurred in BLM-induced mice. However, treatment with CA and SB markedly reduced collagen deposition (Figures 1(b) and 1(f), $P < 0.01$). Collagen I is one of the major collagen proteins of the extracellular matrix, which is an important biomarker of pulmonary fibrosis. The expression of collagen I was tested by immunohistochemistry. Compared with that in the NC group, the expression of collagen I was significantly higher in the BLM group. By contrast, the expression of collagen I was reduced in the lung tissues of the CA group and SB group (Figure 1(c)). Taken together, our data indicates that CA was effective against the progression of pulmonary fibrosis.

3.2. The Effect of CA on Oxidant/Antioxidant Markers in BLM-Induced Pulmonary Fibrosis. Oxidative stress is an important contributor to the pathogenesis of pulmonary fibrosis. The activities of antioxidant factors, SOD ($P < 0.01$) and TAC ($P < 0.01$), in the serum of BLM-induced mice were significantly lower than that of the NC group, while CA

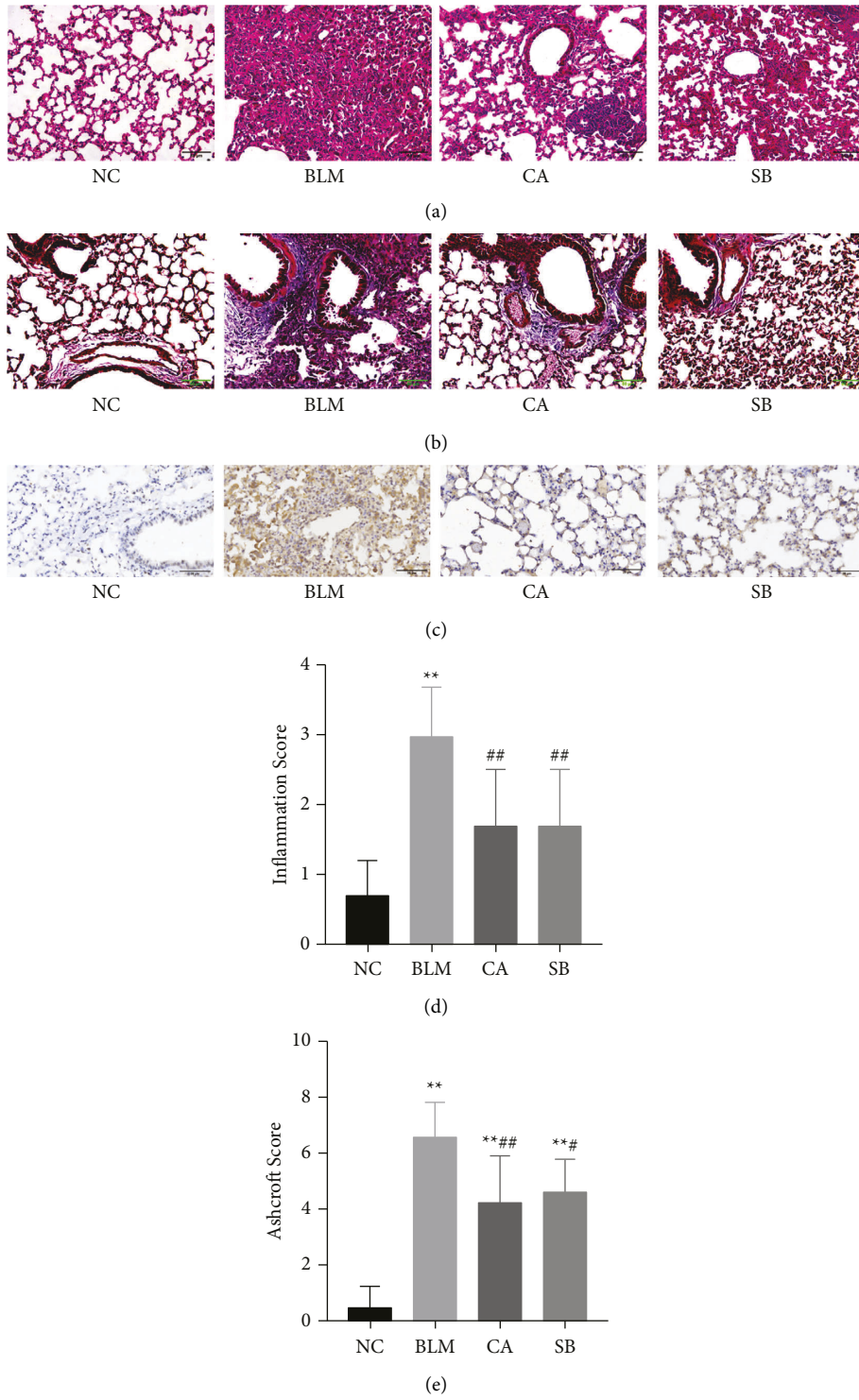


FIGURE 1: Continued.

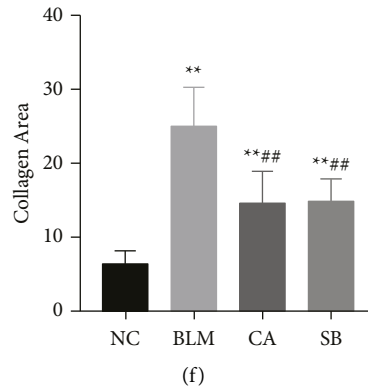


FIGURE 1: Effects of CA on BLM-induced pulmonary fibrosis. (a, b) Representative images of HE staining (200 \times) and Masson staining (200 \times). (c) Immunohistochemistry assays for collagen I (200 \times). (d–f) Quantitative analysis of inflammation score and Ashcroft score based on HE staining, and collagen area based on Masson staining assays. ** $P < 0.01$ compared with the NC group; # $P < 0.05$, ## $P < 0.01$ compared with the BLM group.

administration was observed to increase both SOD ($P < 0.01$) and TAC ($P < 0.01$) levels (Figures 2(b) and 2(c)). In addition, the level of serum MDA, an index of lipid peroxidation was significantly decreased in the CA group compared with the BLM group (Figure 2(a), $P < 0.05$). The Nrf2 and HO-1 are excellent indicators of oxidation and antioxidation processes. This study shows that the relative expression of Nrf2 mRNA expression was decreased with BLM treatment ($P < 0.01$), while CA ($P < 0.01$) and SB ($P < 0.01$) could help increase Nrf2 mRNA expression in the lung (Figure 2(d)). HO-1 was detected by western blotting. BLM administration appears to decrease HO-1 expression, but it was not significant compared to the NC group. In addition, the HO-1 expression in BLM-induced mice was significantly increased with CA ($P < 0.05$) and SB ($P < 0.01$), when compared to the BLM group. In summary, these data demonstrate that CA alleviated the oxidative stress induced by BLM.

3.3. The Effect of CA on Apoptosis in BLM-Induced Pulmonary Fibrosis. Oxidative stress generally induces apoptosis. Therefore, the expression of apoptosis-related markers was also measured. Bcl-2 is an antiapoptotic protein while Bax enhances apoptosis. We found that the expression of Bcl-2 in the BLM group was decreased as compared to the NC group ($P < 0.01$), while CA treatment could restore Bcl-2 expression ($P < 0.01$). Moreover, Bax expression was much activated in the BLM group ($P < 0.01$), while CA treatment ($P < 0.01$) noticeably decreased Bax content (Figures 2(a) and 2(b)). The overexpression of XIAP could decrease apoptosis. While BLM was shown to inhibit XIAP expression ($P < 0.01$), a nonsignificant recovery of XIAP expression was observed in the CA group. HK-2 is also an antiapoptotic protein. HK-2 downregulation by BLM was confirmed in the lung tissue by immunohistochemical staining, while CA was observed to significantly increase HK-2 expression. These data suggest that CA protects against pulmonary fibrosis by inhibiting apoptosis (see Figure 3).

3.4. The Effect of CA on Autophagy in BLM-Induced Pulmonary Fibrosis. To explore whether CA improved pulmonary fibrosis via autophagy, we measured the expression of autophagy-related proteins in fibrotic lung tissues. As shown in Figures 4(a)–4(c), the level of beclin 1 in the BLM group was much lower than that of the NC group ($P < 0.01$), but was increased with SB treatment ($P < 0.01$). The level of PINK1 in the BLM group was higher than that of the NC group ($P < 0.01$), and interestingly, the expression level of PINK1 was further elevated by CA ($P < 0.01$). Unexpectedly, no significant differences in LC3-II and LC3-II/LC3-I were observed between the NC and BLM groups. Nevertheless, CA significantly increased ($P < 0.01$) the conversion of LC3-I to LC3-II (Figures 4(d) and 4(e)). p62 accumulation levels are proportional to the autophagic impairment. Compared with the NC group, the expression level of p62 in the BLM group was significantly increased ($P < 0.01$). After treatment with CA ($P < 0.01$) and SB ($P < 0.01$), p62 expression was obviously decreased (Figure 4(f)). p62 immunohistochemical staining was found consistent with western blot analysis (Figure 4(g)). The morphological changes of the lung tissue were observed using TEM. Compared with the NC group, the cells from the BLM group exhibited few autophagic vesicles, while numerous mitochondria were swollen and enlarged (Figure 5). After administration of CA and SB, the numbers of intracellular autophagosome and autolysosome were increased. Taken together, this data indicated that CA promotes autophagy, which may be responsible for its effects in the alleviation of pulmonary fibrosis.

3.5. Effect of CA on Lysosome Injury in BLM-Induced Pulmonary Fibrosis. Lysosomes are the degradation centres of the autophagy pathway. In our study, we used LAMP1, legumain, and TFEB to monitor lysosomal function. Compared with the NC group, the expression level of LAMP1 was inhibited in the BLM group ($P < 0.05$), but significantly upregulated in both CA ($P < 0.01$) and SB ($P < 0.01$) groups. As shown in Figure 6(c), the expression level of legumain in the BLM group was increased ($P < 0.01$),

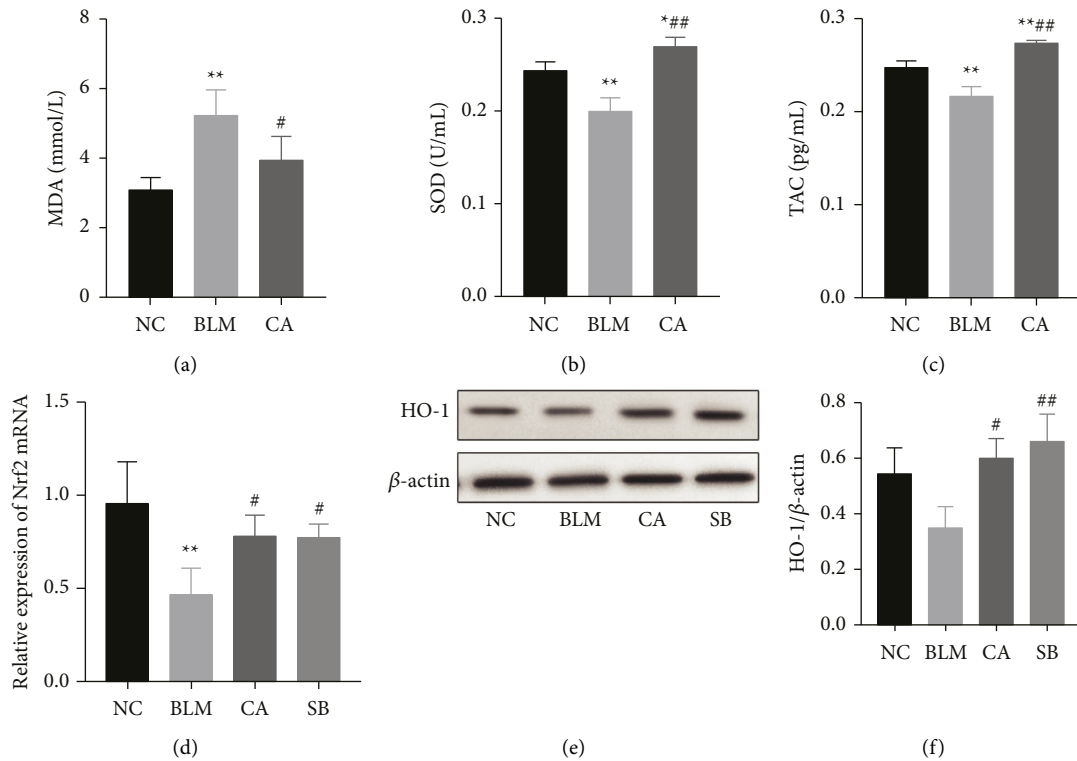


FIGURE 2: Effects of CA on oxidative stress. Total serum levels of (a) MDA, (b) SOD, and (c) TAC as measured through ELISA. (d) Relative mRNA expression of Nrf2. (e) Protein levels of HO-1. (f) Relative density values of HO-1 expression. ** $P < 0.01$, compared with the NC group, # $P < 0.05$, ## $P < 0.01$, compared with the BLM group.

while treatment with CA decreased legumain protein expression ($P < 0.05$). However, SB administration failed to decrease the expression of legumain. The findings were confirmed by immunohistochemistry of legumain (Figure 6(e)). TFEB is the master regulator of lysosome biogenesis. TFEB mRNA was decreased after BLM administration ($P < 0.01$). However, CA ($P < 0.01$) and SB ($P < 0.01$) reversed the BLM-induced reduction of TFEB (Figure 6(d)). Overall, CA alleviates BLM-induced lysosomal damage.

4. Discussion

Calycosin, the most abundantly found isoflavone in *Astragalus*, is a promising antifibrotic agent. It showed promising antioxidant [19], anti-inflammatory [20], and antiapoptotic abilities [21]. Many studies have demonstrated that CA presents as a promising drug for the treatment of organ fibrosis. CA has the potential to be developed into an antifibrotic drug. Zhang et al. suggested that CA mitigated liver fibrosis induced by intraperitoneal injection of CCl₄ by reducing oxidative stress via JAK-STAT3 pathway [22]. Elsherbiny et al. indicated that CA ameliorated renal glomerulosclerosis and interstitial fibrosis in diabetes via modulating oxidative stress by IL33/ST2 signaling [23]. Wang et al. reported that CA significantly inhibited the expression and deposition of collagen I and collagen III in cardiac fibrosis [24]. The cardioprotective effects of CA were mediated through upregulations of the PI3K/AKT pathway.

In pulmonary fibrosis, Liu et al. reported that CA treatment ameliorated the severity of the lung tissue damage of the fibrosis mice model induced by BLM [13]. Moreover, CA reduced transforming growth factor- β 1-induced epithelial-mesenchymal transition in AECs. The therapeutic effects of CA were associated with the AKT/GSK3 β pathway. However, further studies are required to elucidate the biological mechanisms underlying the protective effect of CA. In this study, we attempted to explore the protective effects of CA on BLM-induced pulmonary fibrosis via suppressing oxidative stress, apoptosis, and enhancing autophagy.

Pulmonary fibrosis is a progressive fibroproliferative disorder associated with high mortality and poor prognosis. In recent years, natural products have attracted great attention for medicinal purposes, including pulmonary fibrosis. Prior studies have demonstrated that quantities of natural products exert preventive and therapeutic effects on pulmonary fibrosis through various mechanisms. There is increasing evidence that oxidative stress contributes to pathogenesis of pulmonary fibrosis. Our previous study showed that ROS could result in significant damage to alveolar epithelium, favoring the progression of pulmonary fibrosis [25]. The oxidative stress can be estimated by the levels of ROS, MDA, SOD as well as the activity of GSH-Px. Plants are significant sources of natural antioxidants, and the antioxidant activity of phenolic compounds has been widely recognized. Hesperetin [26], adelmidrol [27], and curcumin [28] upregulated the expression of GSH, SOD, and CAT, reduce MDA and ROS production, and suppress bleomycin-

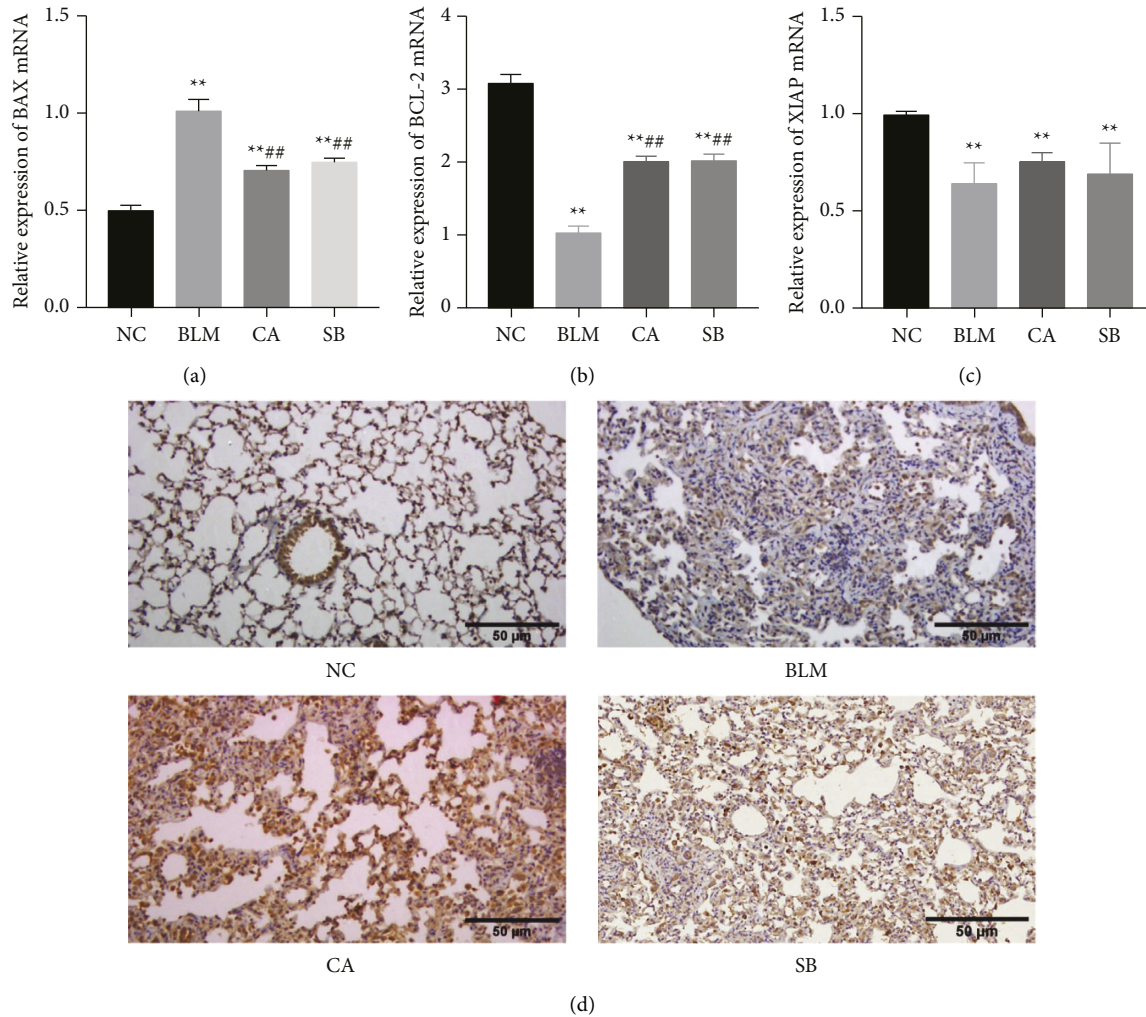


FIGURE 3: Effect of CA on apoptosis-related markers. (a) Bax, (b) Bcl-2, and (c) XIAP mRNA expressions in the lung tissue. (d) Immunohistochemistry assays (200 \times) for HK-2. ** $P < 0.01$ compared with the NC group; # $P < 0.05$, ## $P < 0.01$, compared with the BLM group.

and silica-induced oxidative damage in pulmonary fibrosis. Nrf2 is the master activator for most of the antioxidant enzymes, and its expression was lower in the fibroblasts and myofibroblasts of patients with IPF [29]. Berberine improve pulmonary fibrosis by inducing the activation of Nrf2 to relieve oxidative stress and reduce the deposition of the extracellular matrix [30]. Some studies indicated that CA showed good capability against oxidative stress [31], which protected cells from injury. However, there has been no report about the antioxidant activity of CA in pulmonary fibrosis thus far. In the present study, increasing MDA expression and impaired antioxidant enzyme activities of SOD and TAC were observed in pulmonary fibrosis mice. CA reduced MDA levels and increased SOD and TAC activities. HO-1 is a critical downstream antioxidant enzyme of Nrf2. Our results showed that there was a significant increase in the Nrf2 mRNA levels and HO-1 protein levels after CA administration.

As known, AEC injury is an essential first step in the pathogenesis of pulmonary fibrosis. Excessive ROS production can damage cellular components, thus triggering the

apoptosis of AECs [32]. Apoptosis mainly involves two major pathways: the mitochondrial apoptotic pathway and the death receptor pathway. In the mitochondrial apoptosis pathway, apoptosis is the result of downregulation of mitochondrial membrane potential, and cytochrome C is released from mitochondria into the cytosol [33]. Bcl-2 family proteins are key regulators of apoptosis. Bax, one of the Bcl-2 family members, promotes apoptosis by damaging mitochondrial membrane integrity, whereas Bcl-2 inhibits apoptosis by maintaining the integrity of the mitochondrial membrane [34]. The X-linked inhibitor of apoptosis protein has also been implicated in mitochondrial apoptosis [35]. It inhibits apoptosis mainly by interacting directly with caspases to inhibit them. HK-2 is a structural protein of mPTP, which is essential for maintaining the integrity of mitochondrial membrane structure and mitochondrial membrane potential [36]. After baicalin administration, the TUNEL-positive cells of BLM-treated rats were significantly decreased. Moreover, baicalin increased Bcl-2, and suppressed Bax protein expression in rat lung tissues [37]. Glycyrrhizic acid treatment remarkably ameliorated BLM-

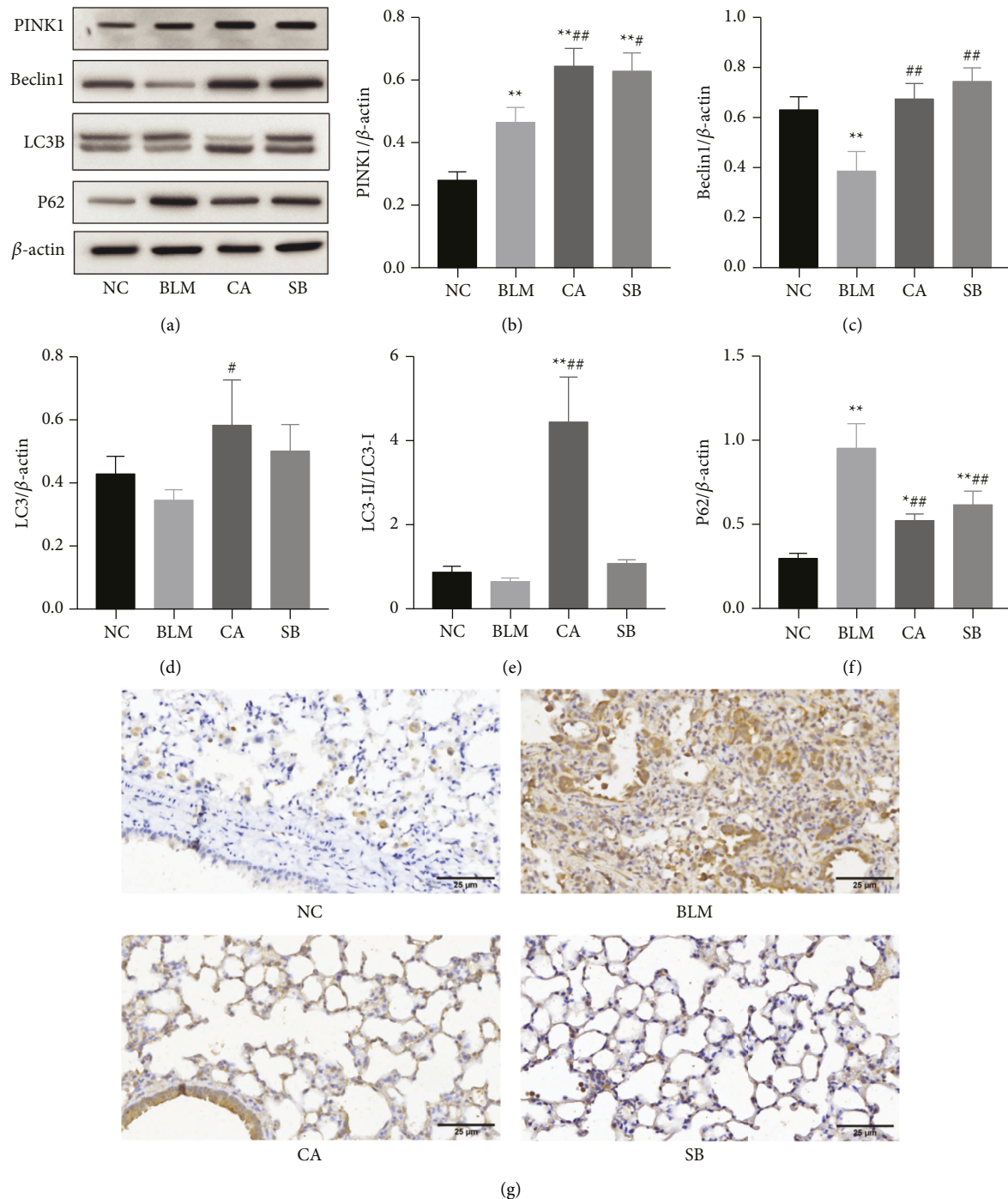


FIGURE 4: Effects of CA on autophagy. (a) Protein levels of PINK1, Beclin1, p62, and LC3II as measured by western blotting. (b–f) Relative density values showing PINK1, Beclin1, LC3-II, LC3-II/LC3-I, and p62 expression. (g) Representative images of immunohistochemical staining (400 \times) for p62. * $P < 0.05$, ** $P < 0.01$, compared with the NC group; # $P < 0.05$, ## $P < 0.01$, compared with BLM group.

induced pulmonary fibrosis by inhibiting proliferation of fibroblast cells and promoted apoptosis in vitro [38]. Based on our research, we found that CA inhibits cell apoptosis by promoting the expression of HK-2 and Bcl-2, and inhibiting the expression of Bax. However, we observed no significant difference in XIAP following CA administration.

Autophagy is a conserved eukaryotic cellular degradation that helps maintain cell metabolism. Excessive

accumulation of ROS induces autophagy, which eliminates damaged mitochondria and alleviates cellular oxidative stress. Studies have shown that autophagy flow is blocked in the lung tissue of patients with IPF [39]. Stimulating autophagy exerts an antifibrotic effect in the experimental fibrosis model by suppressing oxidative stress [40]. Autophagy is related to plenty of autophagy-related genes, among which LC3 and Beclin1 are important autophagic regulators.

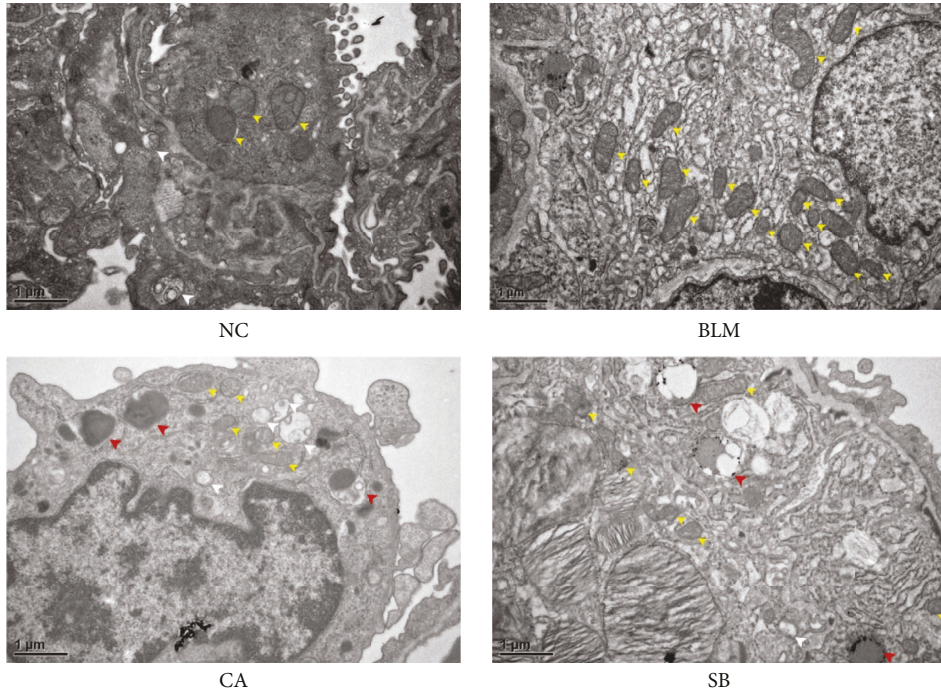


FIGURE 5: Observation of lung tissue of mice using a transmission electron microscope (20,000×). The white arrowheads indicate autophagosomes, the red arrowheads indicate autolysosomes, and the yellow arrowheads indicate mitochondria.

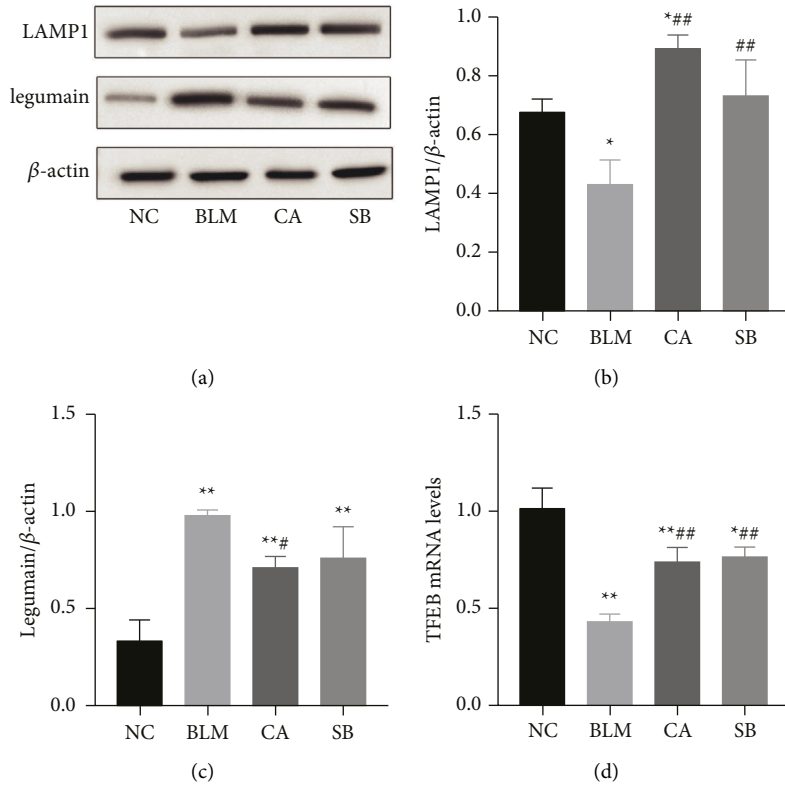


FIGURE 6: Continued.

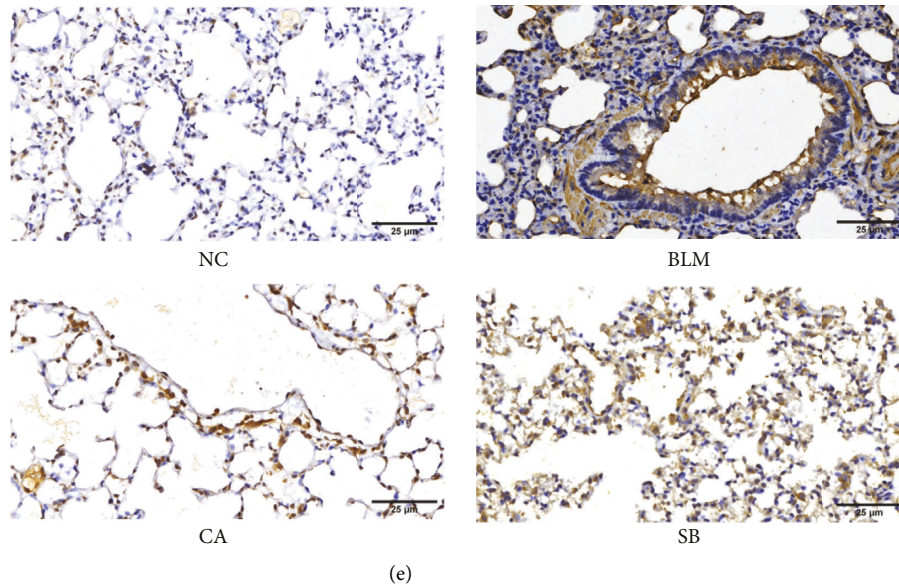


FIGURE 6: Effects of CA on lysosome injury. (a) Protein levels of LAMP1 and legumain as determined by western blotting. Relative density values showing (b) LAMP1 and (c) legumain expressions. (d) mRNA expression of TFEB. (e) Representative images of immunohistochemical staining (400 \times) for legumain. * $P < 0.05$, ** $P < 0.01$, compared with the NC group; # $P < 0.05$, ## $P < 0.01$, compared with the BLM group.

PINK1 is critical for mitochondrial clearance by autophagy, and increased PINK1 indicates smooth autophagy flux [41]. p62 is a substrate of autophagy. Thus, a blockage in autophagy may lead to p62 protein accumulation. It was confirmed that kaempferol partially restored the lipidation of LC3 without affecting p62 expression, increased autophagic flux, and attenuated silica-induced pulmonary fibrosis [42]. Ellagic acid could enhance autophagy formation in myofibroblasts mainly by suppressing the Wnt signaling pathway and promoting apoptosis of myofibroblasts [43]. In this study, CA treatment resulted in a significant downregulation of p62, while the expression of Beclin1, PINK1, and transformation of LC3-I to LC3-II were simultaneously activated. TEM is widely regarded as the gold standard for the qualitative detection of autophagy. Studies have demonstrated that increasing numbers of damaged mitochondria were observed in IPF lung tissue [44]. In line with previous research [45], numerous dysmorphic and enlarged mitochondria, and few autophagic vesicles were observed in lung tissues after BLM administration. Treatment with CA was shown to increase the number of autophagic vesicles.

Lysosome is an intracellular organelle that contains a battery of acid hydrolases. Excessive oxidative stress results in destabilization of lysosomal membrane that causes leakage of lysosomal enzymes, which leads to cell apoptosis [46]. Moreover, the fusion of autophagosome and lysosome is the rate-limiting step of autophagy. Lysosomal defects disturb the degradation of autophagic substrates, leading to the accumulation of autophagosomes [47]. Recent studies demonstrated that silica nanoparticles enhanced autophagosome accumulation by impairing lysosomal degradation via acidification inhibition, leading to the apoptosis of AECs, thus resulting in pulmonary fibrosis [48]. However, little attention has been given to lysosomal disorders in

pulmonary fibrosis. To date, very few studies have explored the activation of lysosome function in BLM-induced pulmonary fibrosis by naturally products. In this study, we utilized LAMP1 and legumain to measure lysosome function. This study showed that BLM intervention significantly downregulated LAMP1 expression and upregulated legumain expression, which was reversed by CA treatment. These findings suggest that BLM intervention induced lysosomal damage, and that CA treatment may protect lysosomal function and promote autophagic substrate degradation. Considering the lack of extensive lysosomal research in pulmonary fibrosis, additional research on lysosomes should be conducted in future studies.

5. Conclusions

In conclusion, this study confirmed that CA improved pulmonary fibrosis induced by BLM in mice, and its mechanism may be related to the inhibition of oxidative stress, activation of the Nrf2/HO-1 pathway, suppression of apoptosis, and upregulation of the autophagy-lysosome pathways. However, in this study, CA was shown to regulate autophagy and apoptosis through multiple pathways [49], and we lack understanding of its potential signaling pathways. Further study would be needed to explore the role of CA in the treatment of idiopathic pulmonary fibrosis.

Abbreviations

AECs:	Alveolar epithelial cells
BAX:	BCL-2-associated X
Bcl-2:	B-cell lymphoma-2
BLM:	Bleomycin
CA:	Calycosin

HE:	Hematoxylin-eosin staining
HO-1:	Heme oxygenase-1
HK-2:	Hexokinase-2
IPF:	Idiopathic pulmonary fibrosis
LAMP1:	Lysosome-associated membrane protein 1
LC3:	Microtubule associated protein 1 light chain 3
MDA:	Malondialdehyde
mtROS:	Mitochondrial reactive oxygen species
Nrf2:	Nuclear factor-erythroid 2-related factor 2
PINK1:	PTEN induced putative kinase 1
SQSTM1/	Sequestosome
p62:	
SOD:	Superoxide dismutase
TAC:	Total antioxidant capacity
TFEB:	Transcription factor EB
TEM:	Transmission electron microscope
XIAP:	X-linked inhibitor of apoptosis protein.

Data Availability

The data are available on request.

Conflicts of Interest

The authors declare that they have no conflicts of interest.

Acknowledgments

This study was supported by the Beijing Natural Science Foundation (No. 7202118) and National Natural Science Foundation of China (No. 81573970).

References

- [1] U. Costabel, "The changing treatment landscape in idiopathic pulmonary fibrosis," *European Respiratory Review*, vol. 24, pp. 65–68, 2015.
- [2] M. Ghazipura, M. J. Mammen, D. D. Herman et al., "Nintedanib in progressive pulmonary fibrosis: a systematic review and meta-analysis," *Annals of the American Thoracic Society*, vol. 19, 2022.
- [3] G. Raghu, M. Remy-Jardin, L. Richeldi et al., "Idiopathic pulmonary fibrosis (an update) and progressive pulmonary fibrosis in adults: an official ATS/ERS/JRS/ALAT clinical practice guideline," *American Journal of Respiratory and Critical Care Medicine*, vol. 205, no. 9, pp. e18–e47, 2022.
- [4] D. Wu, M. Liang, H. Dang, F. Fang, F. Xu, and C. Liu, "Hydrogen protects against hyperoxia-induced apoptosis in type II alveolar epithelial cells via activation of PI3K/Akt/Foxo3a signaling pathway," *Biochemical and Biophysical Research Communications*, vol. 495, no. 2, pp. 1620–1627, 2018.
- [5] Y. Kurita, J. Araya, S. Minagawa et al., "Pirfenidone inhibits myofibroblast differentiation and lung fibrosis development during insufficient mitophagy," *Respiratory Research*, vol. 18, no. 1, p. 114, 2017.
- [6] M. Xiong, Y. Zhao, H. Mo, H. Yang, F. Yue, and K. Hu, "Intermittent hypoxia increases ROS/HIF-1 α related oxidative stress and inflammation and worsens bleomycin-induced pulmonary fibrosis in adult male C57BL/6 mice," *International Immunopharmacology*, vol. 100, Article ID 108165, 2021.
- [7] Z. Ding, X. Wu, Y. Wang et al., "Melatonin prevents LPS-induced epithelial-mesenchymal transition in human alveolar epithelial cells via the GSK-3 β /Nrf2 pathway," *Biomedicine & Pharmacotherapy*, vol. 132, Article ID 110827, 2020.
- [8] H. Yang, L. Wang, M. Yang, J. Hu, E. Zhang, and L. Peng, "Oridonin attenuates LPS-induced early pulmonary fibrosis by regulating impaired autophagy, oxidative stress, inflammation and EMT," *European Journal of Pharmacology*, vol. 923, Article ID 174931, 2022.
- [9] D. D. A. F. Caldeira, D. J. Weiss, P. R. M. Rocco, P. L. Silva, and F. F. Cruz, "Mitochondria in focus: from function to therapeutic strategies in chronic lung diseases," *Frontiers in Immunology*, vol. 12, Article ID 782074, 2021.
- [10] K. Wang, T. Zhang, Y. Lei et al., "Identification of ANXA2 (annexin A2) as a specific bleomycin target to induce pulmonary fibrosis by impeding TFEB-mediated autophagic flux," *Autophagy*, vol. 14, no. 2, pp. 269–282, 2018.
- [11] S. Cabrera, M. Maciel, I. Herrera et al., "Essential role for the ATG4B protease and autophagy in bleomycin-induced pulmonary fibrosis," *Autophagy*, vol. 11, no. 4, pp. 670–684, 2015.
- [12] M. S. Kim, A. R. Baek, J. H. Lee et al., "IL-37 attenuates lung fibrosis by inducing autophagy and regulating TGF- β 1 production in mice," *The Journal of Immunology*, vol. 203, no. 8, pp. 2265–2275, 2019.
- [13] X. Liu, Y. Shao, X. Zhang, X. Ji, M. Xie, and H. Liu, "Calycosin attenuates pulmonary fibrosis by the epithelial-mesenchymal transition repression upon inhibiting the AKT/GSK3 β / β -catenin signaling pathway," *Acta Histochemica*, vol. 123, no. 5, Article ID 151746, 2021.
- [14] J. Zhao, Y. Ren, Y. Qu, W. Jiang, and C. Lv, "Pharmacodynamic and pharmacokinetic assessment of pulmonary rehabilitation mixture for the treatment of pulmonary fibrosis," *Scientific Reports*, vol. 7, no. 1, p. 3458, 2017.
- [15] J. Chen, J. Lu, B. Wang et al., "Polysaccharides from *Dendrobium officinale* inhibit bleomycin-induced pulmonary fibrosis via the TGF β 1-Smad2/3 axis," *International Journal of Biological Macromolecules*, vol. 118, pp. 2163–2175, 2018.
- [16] C. Gurrieri, F. Piazza, M. Gnoato et al., "3-(2, 4-dichlorophenyl)-4-(1-methyl-1H-indol-3-yl)-1H-pyrrole-2, 5-dione (SB216763), a glycogen synthase kinase-3 inhibitor, displays therapeutic properties in a mouse model of pulmonary inflammation and fibrosis," *Journal of Pharmacology and Experimental Therapeutics*, vol. 332, no. 3, pp. 785–794, 2010.
- [17] S. Dai, F. Zhou, J. Sun, and Y. Li, "NPD1 enhances autophagy and reduces hyperphosphorylated tau and amyloid- β 42 by inhibiting GSK3 β activation in N2a/APP695swe cells," *Journal of Alzheimer's Disease*, vol. 84, no. 2, pp. 869–881, 2021.
- [18] K. Wang, Y. Wang, Y. Cao et al., "Lumican is elevated in the lung in human and experimental acute respiratory distress syndrome and promotes early fibrotic responses to lung injury," *Journal of Translational Medicine*, vol. 20, no. 1, p. 392, 2022.
- [19] L. Zhang, C. Fan, H. C. Jiao et al., "Calycosin alleviates doxorubicin-induced cardiotoxicity and pyroptosis by inhibiting NLRP3 inflammasome activation," *Oxidative Medicine and Cellular Longevity*, vol. 2022, pp. 1–15, 2022.
- [20] C. Y. Lu, C. H. Day, C. H. Kuo et al., "Calycosin alleviates H₂O₂-induced astrocyte injury by restricting oxidative stress through the Akt/Nrf2/HO-1 signaling pathway," *Environmental Toxicology*, vol. 37, no. 4, pp. 858–867, 2022.

- [21] Y. Liu, X. J. Piao, W. T. Xu et al., "Calycosin induces mitochondrial-dependent apoptosis and cell cycle arrest, and inhibits cell migration through a ROS-mediated signaling pathway in HepG2 hepatocellular carcinoma cells," *Toxicology in Vitro*, vol. 70, Article ID 105052, 2021.
- [22] M. Zhang, Y. Wang, G. Zhu, C. Sun, and J. Wang, "Hepatoprotective effect and possible mechanism of phytoestrogen calycosin on carbon tetrachloride-induced liver fibrosis in mice," *Naunyn-Schmiedeberg's Archives of Pharmacology*, vol. 394, no. 1, pp. 189–204, 2021.
- [23] N. M. Elsherbiny, E. Said, H. Atef, and S. A. Zaitone, "Renoprotective effect of calycosin in high fat diet-fed/STZ injected rats: effect on IL-33/ST2 signaling, oxidative stress and fibrosis suppression," *Chemico-Biological Interactions*, vol. 315, Article ID 108897, 2020.
- [24] X. Wang, W. Li, Y. Zhang et al., "Calycosin as a novel PI3K activator reduces inflammation and fibrosis in heart failure through AKT-IKK/STAT3 Axis," *Frontiers in Pharmacology*, vol. 13, Article ID 828061, 2022.
- [25] X. Gu, Q. Long, W. Wei et al., "Number 2 feibi recipe inhibits H₂O₂-mediated oxidative stress damage of alveolar epithelial cells by regulating the balance of mitophagy/apoptosis," *Frontiers in Pharmacology*, vol. 13, Article ID 830554, 2022.
- [26] S. Li, L. Shao, J. Fang et al., "Hesperetin attenuates silica-induced lung injury by reducing oxidative damage and inflammatory response," *Experimental and Therapeutic Medicine*, vol. 21, no. 4, p. 297, 2021.
- [27] R. Fusco, M. Cordaro, T. Genovese et al., "Adelmidrol: a new promising antioxidant and anti-inflammatory therapeutic tool in pulmonary fibrosis," *Antioxidants*, vol. 9, no. 7, p. 601, 2020.
- [28] L. R. Rodriguez, S. N. Bui, R. T. Beuschel et al., "Curcumin induced oxidative stress attenuation by N-acetylcysteine co-treatment: a fibroblast and epithelial cell in-vitro study in idiopathic pulmonary fibrosis," *Molecular Medicine*, vol. 25, no. 1, p. 27, 2019.
- [29] Y. Y. Han, X. Gu, C. Y. Yang et al., "Protective effect of dimethyl itaconate against fibroblast-myofibroblast differentiation during pulmonary fibrosis by inhibiting TXNIP," *Journal of Cellular Physiology*, vol. 236, no. 11, pp. 7734–7744, 2021.
- [30] Q. Zeng, T. Zhou, F. Zhao et al., "p62-Nrf2 regulatory loop mediates the anti-pulmonary fibrosis effect of bergenin," *Antioxidants*, vol. 11, no. 2, p. 307, 2022.
- [31] J. Zhai, L. Tao, S. Zhang et al., "Calycosin ameliorates doxorubicin-induced cardiotoxicity by suppressing oxidative stress and inflammation via the sirtuin 1-NOD-like receptor protein 3 pathway," *Phytotherapy Research*, vol. 34, pp. 649–659, 2020.
- [32] T. Parimon, C. Yao, B. R. Stripp, P. W. Noble, and P. Chen, "Alveolar epithelial type II cells as drivers of lung fibrosis in idiopathic pulmonary fibrosis," *International Journal of Molecular Sciences*, vol. 21, no. 7, p. 2269, 2020.
- [33] C. C. Chua, J. Gao, Y. S. Ho et al., "Over-expression of a modified bifunctional apoptosis regulator protects against cardiac injury and doxorubicin-induced cardiotoxicity in transgenic mice," *Cardiovascular Research*, vol. 81, no. 1, pp. 20–27, 2009.
- [34] H. C. Chen, M. Kanai, A. Inoue-Yamauchi et al., "An interconnected hierarchical model of cell death regulation by the BCL-2 family," *Nature Cell Biology*, vol. 17, no. 10, pp. 1270–1281, 2015.
- [35] M. Daoud, P. N. Broxtermann, F. Schorn et al., "XIAP promotes melanoma growth by inducing tumour neutrophil infiltration," *EMBO Reports*, vol. 23, no. 6, Article ID e53608, 2022.
- [36] C. Duan, L. Kuang, C. Hong et al., "Mitochondrial Drp1 recognizes and induces excessive mPTP opening after hypoxia through BAX-PiC and LRRK2-HK2," *Cell Death & Disease*, vol. 12, no. 11, p. 1050, 2021.
- [37] H. Zhao, C. Li, L. Li et al., "Baicalin alleviates bleomycin-induced pulmonary fibrosis and fibroblast proliferation in rats via the PI3K/AKT signaling pathway," *Molecular Medicine Reports*, vol. 21, no. 6, pp. 2321–2334, 2020.
- [38] L. Gao, H. Tang, H. He et al., "Glycyrrhizic acid alleviates bleomycin-induced pulmonary fibrosis in rats," *Frontiers in Pharmacology*, vol. 6, p. 215, 2015.
- [39] J. Araya, J. Kojima, N. Takasaka et al., "Insufficient autophagy in idiopathic pulmonary fibrosis," *American Journal of Physiology - Lung Cellular and Molecular Physiology*, vol. 304, no. 1, pp. L56–L69, 2013.
- [40] Y. Zhang, W. Huang, Z. Zheng et al., "Cigarette smoke-inactivated SIRT1 promotes autophagy-dependent senescence of alveolar epithelial type 2 cells to induce pulmonary fibrosis," *Free Radical Biology and Medicine*, vol. 166, pp. 116–127, 2021.
- [41] K. Liu, Z. Liu, Z. Liu et al., "Manganese induces S-nitrosylation of PINK1 leading to nerve cell damage by repressing PINK1/Parkin-mediated mitophagy," *Science of the Total Environment*, vol. 834, Article ID 155358, 2022.
- [42] H. Liu, H. Yu, Z. Cao et al., "Kaempferol modulates autophagy and alleviates silica-induced pulmonary fibrosis," *DNA and Cell Biology*, vol. 38, no. 12, pp. 1418–1426, 2019.
- [43] X. Li, K. Huang, X. Liu et al., "Ellagic acid attenuates BLM-induced pulmonary fibrosis via inhibiting Wnt signaling pathway," *Frontiers in Pharmacology*, vol. 12, Article ID 639574, 2021.
- [44] A. S. Patel, J. W. Song, S. G. Chu et al., "Epithelial cell mitochondrial dysfunction and PINK1 are induced by transforming growth factor-beta1 in pulmonary fibrosis," *PLoS One*, vol. 10, no. 3, Article ID e0121246, 2015.
- [45] M. Bueno, Y. C. Lai, Y. Romero et al., "PINK1 deficiency impairs mitochondrial homeostasis and promotes lung fibrosis," *Journal of Clinical Investigation*, vol. 125, no. 2, pp. 521–538, 2015.
- [46] H. Wang, N. Wang, D. Xu et al., "Oxidation of multiple MiT/TFE transcription factors links oxidative stress to transcriptional control of autophagy and lysosome biogenesis," *Autophagy*, vol. 16, no. 9, pp. 1683–1696, 2020.
- [47] Y. Yu, L. Wang, F. Delguste et al., "Advanced glycation end products receptor RAGE controls myocardial dysfunction and oxidative stress in high-fat fed mice by sustaining mitochondrial dynamics and autophagy-lysosome pathway," *Free Radical Biology and Medicine*, vol. 112, pp. 397–410, 2017.
- [48] X. He, S. Chen, C. Li et al., "Trehalose alleviates crystalline silica-induced pulmonary fibrosis via activation of the TFEB-mediated autophagy-lysosomal system in alveolar macrophages," *Cells*, vol. 9, no. 1, p. 122, 2020.
- [49] G. Gong, Y. Zheng, Y. Yang, Y. Sui, and Z. Wen, "Pharmaceutical values of calycosin: one type of flavonoid isolated from Astragalus," *Evidence-based Complementary and Alternative Medicine*, vol. 2021, pp. 1–9, 2021.